

How reduced vacuum pumping capability in a coating chamber affects the laser damage resistance of $\text{HfO}_2/\text{SiO}_2$ antireflection and high reflection coatings

Ella S. Field*, John C. Bellum, Damon E. Kletecka
 Sandia National Laboratories, PO Box 5800, MS 1191, Albuquerque, NM, 87185
 Contact: efield@sandia.gov

ABSTRACT

Optical coatings with the highest laser damage thresholds rely on clean conditions in the vacuum chamber during the coating deposition process. A low base pressure in the coating chamber, as well as the ability of the vacuum system to maintain the required pressure during deposition, are important aspects of limiting the amount of defects in an optical coating that could induce laser damage. Our large optics coating chamber at Sandia National Laboratories normally relies on three cryo pumps to maintain low pressures for e-beam coating processes. However, on occasion, one or more of the cryo pumps have been out of commission. In light of this circumstance, we decided to explore how deposition under compromised vacuum conditions resulting from the use of only one or two cryo pumps affects the laser-induced damage thresholds of optical coatings. The coatings of this study consist of HfO_2 and SiO_2 layer materials and include antireflection coatings for 527 nm at normal incidence, and high reflection coatings for 527 nm, 45° angle of incidence (AOI), in P-polarization (P-pol).

1. INTRODUCTION

The large optics coating system at Sandia National Laboratories uses e-beam evaporation to produce optical coatings with high resistance to laser damage for the kJ-class Z-Backlighter laser system^{1,2}. The coating system has been in operation since 2005 for the production of antireflection, high reflection, polarizer, and dichroic coatings on meter-class optics, using mainly HfO_2 and SiO_2 coating materials³⁻⁷.

Producing an optical coating with a high laser-induced damage threshold (LIDT) involves many variables, including the substrate preparation⁸⁻¹⁰, coating material selections^{5,6,11}, deposition method¹², pulse duration of the laser¹³, and likely the pressures maintained during deposition. This study concerns pressure; specifically, the consequences of losing some vacuum pumping capability during a coating deposition. This is a real concern of ours because, on rare occasions, a vacuum pump requires maintenance and needs to be taken out of service while a coating deposition is taking place. Until this study was conducted, we did not know how the loss of a vacuum pump would impact the LIDT of our coatings.

The vacuum conditions in our 2.3 m X 2.3 m X 1.8 m coating chamber are maintained by 3 cryo pumps, which provide base pressures as low as 5e-7 Torr. When a cryo pump is out of service during a coating deposition, the remainder of the deposition is supported by just 2 cryo pumps, or in the worst case, 1 cryo pump. In order to understand how the loss of one or two cryo pumps affects the LIDT of an optical

coating, this study replicated those conditions with two of our most common coatings. These coatings are antireflection (AR) coatings (for 527 nm, 0° AOI), and high reflection (HR) coatings (for 527 nm, 45° AOI, P-pol). In practice, the HR coating is used for fold mirrors, while the AR coating is used for transmissive optics (debris shields, vacuum windows, and lenses) for dual wavelengths of 527 nm/1054 nm. We have reported on the LIDT results of the AR coating at 532 nm and 1064 nm^{2,4}. For this study, we deposited the AR and HR coatings with vacuum in the chamber provided by one, two, and three cryo pumps, and then had LIDT measurements performed on each coating.

2. EXPERIMENTAL METHOD

The AR coatings were a standard 4-layer design, and the HR coatings were a 34-layer quarter-wave design, with the final SiO₂ layer being a half-wave thick to improve the LIDT¹³.

The SiO₂ layers were produced from the evaporation of SiO₂ granules (1-3 mm in size) in a rotating dish, with a deposition rate of 7 Å/s. The HfO₂ layers were produced by evaporating hafnium metal, with an oxygen backfill resulting in a total pressure in the chamber of 1.1e-4 Torr. In the AR coatings, the first HfO₂ layer (layer #1) was deposited at a rate of 1 Å/s and the second HfO₂ layer (layer #3) was deposited at a rate of 2 Å/s. In the HR coatings, the HfO₂ layers were deposited at a rate of 3 Å/s. Both the AR and HR coatings were deposited at 200° C.

Each coating was deposited onto a 50 mm diameter, 10 mm thick, optically polished fused silica substrate. Each substrate was prepared according to our standard cleaning method⁸ immediately before they were loaded into the coating chamber.

Normally, ion-assisted deposition (IAD) is required to produce “thick” HR coatings without stress problems if the substrate is large and made of fused silica². However, because the substrates in this study are small, we did not take the precaution of producing the HR coatings with IAD.

The coating system uses planetary rotation and masking to maintain coating uniformity. Quartz crystal monitoring with a single crystal is used for layer thickness control. Before each coating took place, the base pressure in the coating chamber was near 3e-6 Torr for the AR coatings, and 5e-6 Torr for the HR coatings. The pressure in the coating chamber was determined using a calibrated ion gauge (model: 370 Stabil-ion gauge, from Granville Phillips).

A summary of the coating designs and deposition conditions are shown below in Table 1.

Table 1: Summary of Coating Designs and Deposition Conditions

AR Coating for 527 nm, 0° AOI	HR Coating for 527 nm, 45° AOI, P-polarization
4 layers → 565.3 nm thick	34 layers – Quarter-wave design with outermost layer ~½ wave SiO ₂ → 3194.7 nm thick
SiO ₂ deposition rate: 7 Å/s deposition rate	SiO ₂ deposition rate: 7 Å/s
HfO ₂ deposition rate: 1 Å/s (layer 1), 2 Å/s (layer 3)	HfO ₂ deposition rate: 3 Å/s
Deposition time: 46 min.	Deposition time: 4 hrs 53 min.
Base pressure: ~3e-6 Torr	Base Pressure ~5e-6 Torr

After the coatings were produced, the substrates were washed with detergent and DI water according to our standard cleaning method⁸, and then sent to the laser damage testing facility. The coatings were tested about 1 month after deposition. An aging effect in e-beam deposited coatings results in a permanent but small spectral shift to longer wavelength. Our coatings, especially the thicker ones for HR, have a tendency to age most within the first week of being deposited, while the thinner AR coatings hardly age at all. The LIDT tests were conducted after the aging effects appeared to have finished.

3. LASER DAMAGE TESTING PROTOCOL

The LIDTs were measured at 532 nm and 0° AOI for the AR coatings and at 532 nm and 45° AOI in Ppol for the HR coatings. The laser damage measurements were conducted by Spica Technologies, Inc.¹⁵ using the NIF-MEL protocol¹⁶. In this protocol, the coated surface of the test optic first undergoes an alcohol drag-wipe cleaning step. Then, single transverse mode, multi-longitudinal mode laser pulses of 3.5 ns duration and produced at a 5 Hz repetition rate in a 1 mm diameter collimated beam are incident one at a time per site in a raster scan composed of ~ 2500 sites over a 1 cm² area. In the raster scan, the laser spot overlaps itself from one site to the next at 90% of its peak intensity radius. The laser fluence typically starts at 1 J/cm² in the cross section of the laser beam. After testing the 2500 sites at 1 J/cm², the fluence is increased in a 3 J/cm² increment and the 2500 sites are tested again. This progression repeats until the damage threshold fluence is reached.

The NIF-MEL procedure is essentially an N-on-1 test at each of the 2500 sites. Laser damage is identified as some type of melt or crater that alters the coated surface, but in some cases the damage stabilizes as a damage site that does not propagate – that is, grow in size – as the laser fluence increases. These non-propagating (NP) damage sites tend to be caused by the interaction of the laser field with nano-defects (pits, nodules, or contamination) in the coating. In other cases, the damage does propagate.

Propagating damage tends to be intrinsic, governed by how the laser field interacts directly with the coating molecules.

According to the NIF-MEL damage criterion, the LIDT is reached at the fluence at which 1 or more propagating damage sites occurs, or the fluence at which the number of NP damage sites accumulates to at least 25, whichever fluence is smaller. The 25 or more NP sites are 1% or more of the 2500 sites tested and constitute about 1% or more of the 1 cm² coating area tested. Our reason for choosing an LIDT test with these damage criteria is the following. We know we cannot tolerate a propagating damage site in the laser beam train because it will quickly develop into catastrophic damage in the form of a large crater in the optic or worse; and 25 or more NP damage sites per cm², while they are benign because they do not grow, are flaws in the coating that scatter about 1% or more of the laser light out of the beam, and that level of loss of laser intensity is unacceptable for us.

4. RESULTS

In this section we discuss how reducing the number of cryo pumps in operation during the coating depositions affects the following: (i) the spectral characteristics of the coatings, (ii) the chamber pressure during depositions, and (iii) the LIDT of the coatings.

Transmission spectra of the coatings were taken with a Perkin Elmer Lambda 950 spectrophotometer. The scans were taken 1 month after the coatings were deposited to account for aging effects, which tend to cause the spectra of e-beam deposited coatings to shift to longer wavelength. The transmission of the AR coatings, as shown in Fig. 1, are practically identical no matter how many cryo pumps were in operation during the deposition. We suspect these AR coatings were too thin for slight changes in coating process parameters to escalate into noticeable problems. On the other hand, the transmission of the HR coatings (Fig. 2) show a slight shift to longer wavelength as the number of cryo pumps in operation decrease. An examination of the pressure in the chamber during deposition helps explain these results.

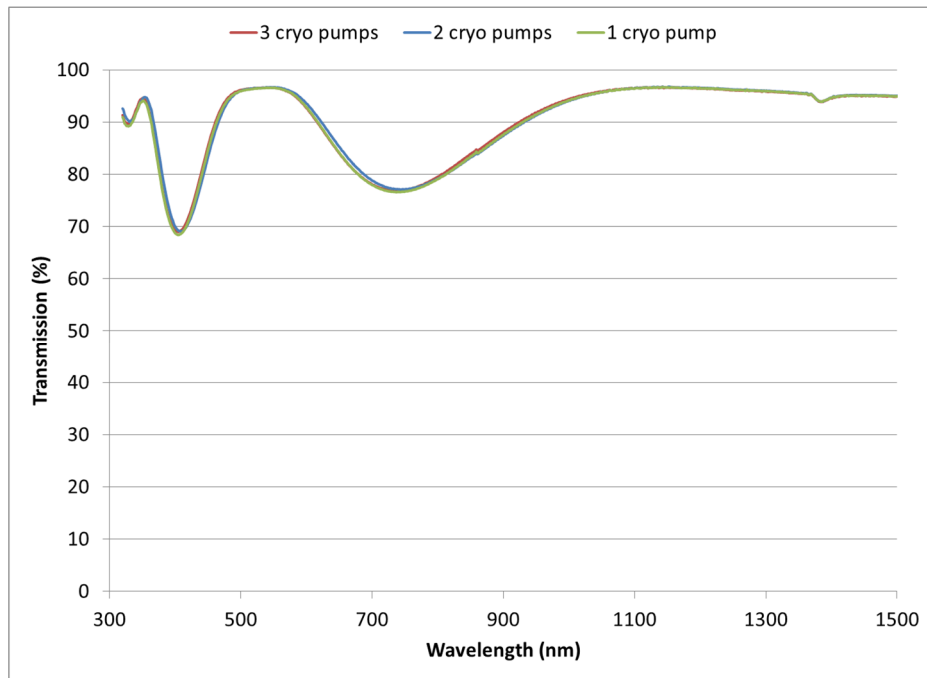


Figure 1: Transmission spectral scans of the AR coatings, taken at 0° AOI.

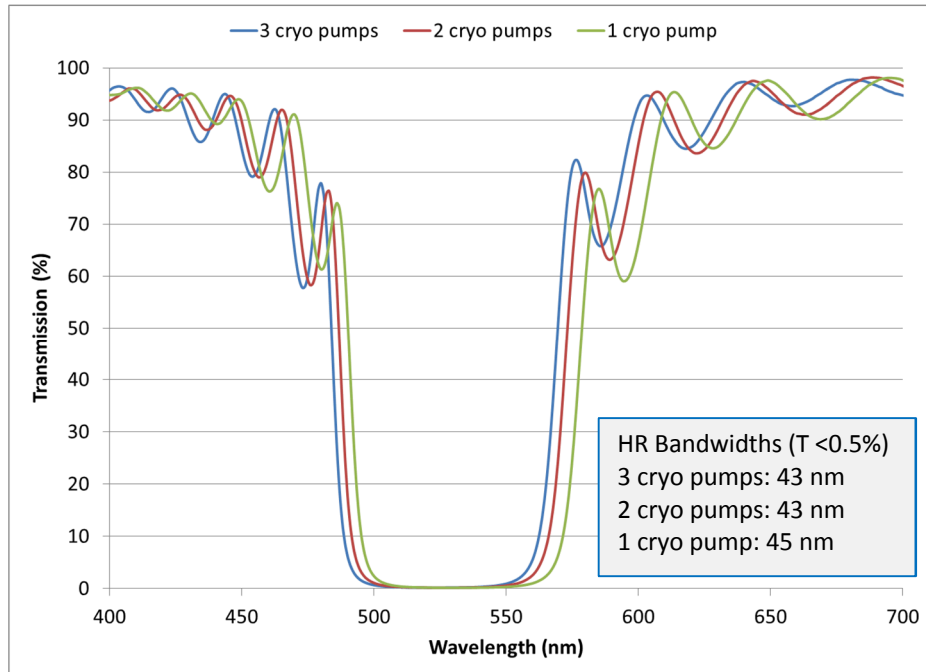


Figure 2: Transmission spectral scans of the HR coatings, taken at 45° AOI, P-pol.

The total pressure in the chamber during the depositions is shown in Fig. 3 for the AR coatings and in Fig. 4 for the HR coatings. Both figures show that fewer cryo pumps lead to higher pressures during SiO_2 deposition, while the pressures maintained during the deposition of HfO_2 are more consistent no matter how many cryo pumps were in operation. The pressure results for SiO_2 are not surprising, since fewer cryo pumps reduce the pumping speed of particles generated by the deposition, causing higher pressures in the coating chamber. HfO_2 layers were deposited with O_2 backfill, managed by a mass flow controller, and it was therefore less apparent at first that fewer cryo pumps cause pressure problems. However, the mass flow controller uses the total pressure in the chamber as feedback, rather than the actual flow rate of O_2 . In other words, the mass flow controller supplies enough O_2 into the chamber so that a certain total pressure is maintained (in this case, $1.1\text{e-}4$ Torr). This means we had no control over the partial pressure of the O_2 backfill, so it is unclear how much O_2 was actually in the chamber. We have reason to be suspicious because the increased pressures during SiO_2 deposition with fewer cryo pumps seem to indicate a slight excess of particles in the chamber that otherwise would not be there if all cryo pumps were operating. This excess of particles likely also exists during HfO_2 deposition when fewer cryo pumps are in operation, and this could lead to lower O_2 partial pressures due to the total pressure being maintained at a constant value. This would cause poorer oxidation of the Hf coating material, and lead to a higher HfO_2 index of refraction. The transmission scans in Fig. 2 indicate that the index of refraction of HfO_2 probably increased because the spectra shift to longer wavelengths and the HR bandwidths increase slightly as fewer cryo pumps are in operation.

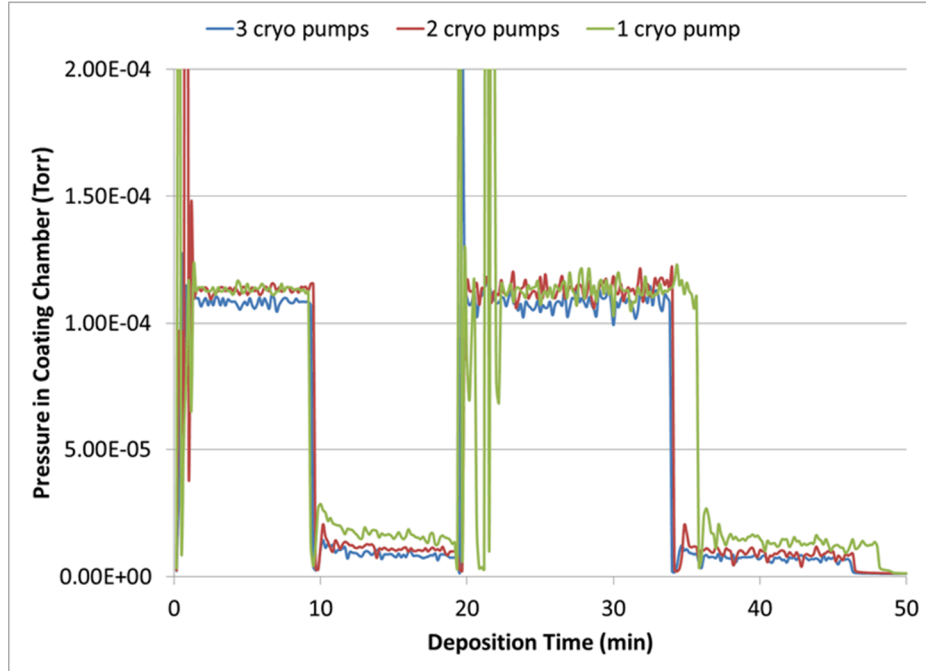


Figure 3: Total pressure in the coating chamber during the deposition of the AR coatings.

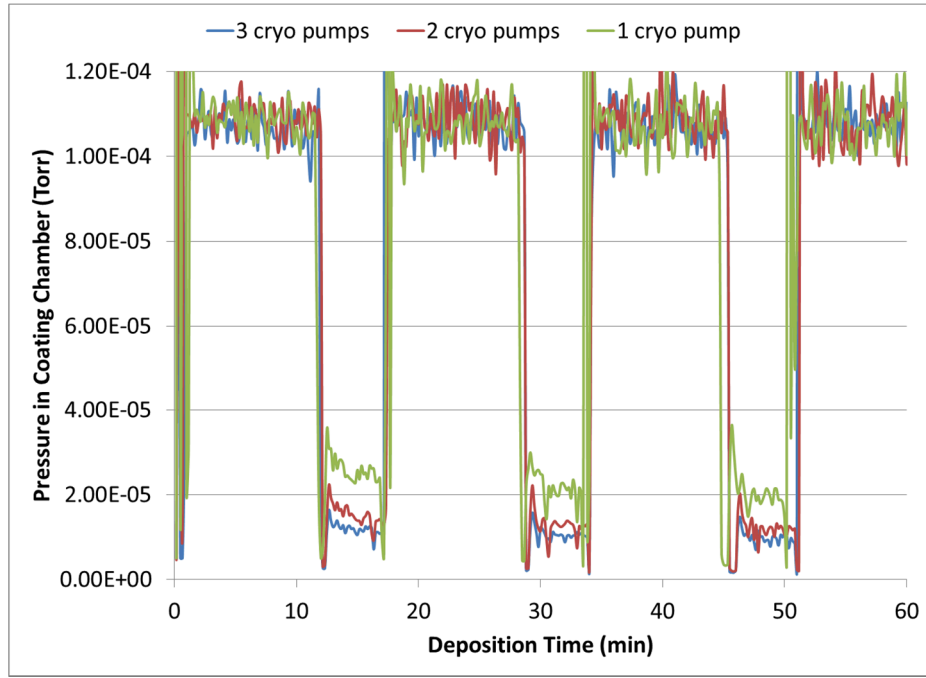


Figure 4: Total pressure in the coating chamber during the deposition of the HR coatings. This figure captures the first 7 layers of the deposition.

The LIDT results of the AR coatings are shown in Fig. 5. They follow a straightforward trend: as the number of cryo pumps in operation decrease, the LIDT also decreases. All coatings reached their LIDT due to the accumulation of 25 or more non-propagating defects, as shown in the plot in Fig. 6. This confirms the importance of vacuum pumping speed in a coating chamber for producing coatings with

the highest resistance to laser damage. The decrease in LIDT is sharpest between the coatings that were produced with 3 and 2 cryo pumps (10.1 J/cm^2 and 7.3 J/cm^2 , respectively, or 2.8 J/cm^2 difference). The difference in LIDT between 2 and 1 cryo pumps is just 0.7 J/cm^2 , which is four times less than the LIDT difference between 3 and 2 cryo pumps in operation. This indicates that the defects causing laser damage are produced mostly by removing just one cryo pump from service, and removing a second cryo pump does not increase the number of defects much beyond what it already was.

The LIDT results for the HR coatings, presented in Fig. 7, follow a less straightforward trend compared to the AR coatings. Fig. 7 shows that the HR coating on BK7 with 3 cryos has the highest LIDT. The number of non-propagating damage sites for each HR coating are plotted in Fig. 8, and this data shows that the coating deposited with 2 cryo pumps damaged due to propagation (with an accumulation of 17 non-propagating damage sites), while the coatings deposited with 1 or 3 cryo pumps damaged due to the accumulation of 25 or more non-propagating damage sites. Uncharacteristically large numbers of these defect-related, non-propagating damage sites are the reason why one of the two coatings deposited with 3 cryo pumps had an unusually low LIDT, but the source of these defects is unknown. Fortunately, we deposited the same HR coating several months before on a substrate that was BK7 rather than fused silica, but had the same surface quality specifications as the fused silica substrates used in this study. The LIDT results of this coating are included in Figs. 7 and 8, and are closer to what we expect for this type of coating (26 J/cm^2). Because this coating also reached its LIDT due to the accumulation of non-propagating defects rather than propagation, the elimination of non-propagating defects is of high importance for increasing the LIDTs of these coatings. The non-propagating defects may be caused by particles in the coating chamber that become trapped in the coating, or perhaps they are a result of Hf in the coating that did not get oxidized. Both of these phenomena are exacerbated by reduced vacuum pumping capability, which slows the pumping speed of particles in the chamber and likely lowers the partial pressure of the O_2 backfill provided during the deposition of HfO_2 .

Unlike the AR coatings, the most drastic drop in LIDT for the HR coatings occurs after 2 cryo pumps are removed from service. In other words, deposition with just one cryo pump causes the greatest number of defects to accumulate in the HR coatings, and this produces the lowest LIDT. This again reinforces the importance of adequate vacuum pumping speed to produce coatings with the highest LIDTs. Accounting for this difference between the AR and HR coatings is probably related to the electric field intensities in these coatings. In the HR coatings, the electric field intensity is highest in only the few outermost layers, and then quenches rapidly within the coating. In the AR coatings, the laser light must penetrate through the entire coating, so the electric field intensity does not quench, and this raises the likelihood of illuminating a defect with high intensity fluence compared to HR coatings. In other words, AR coatings are more susceptible to laser damage compared to HR coatings and we expect defects to play a larger role in influencing the LIDT of AR coatings. However, when conditions are not ideal because of only 1 cryo pump in operation, it is interesting that the LIDTs of the AR and HR coatings are similar (6.6 J/cm^2 and 7.1 J/cm^2 , respectively). We conclude that when vacuum pumping conditions are very poor, neither AR nor HR coatings have an advantage at resisting laser damage, and are equally susceptible to the negative LIDT consequences of defects embedded in the coating.

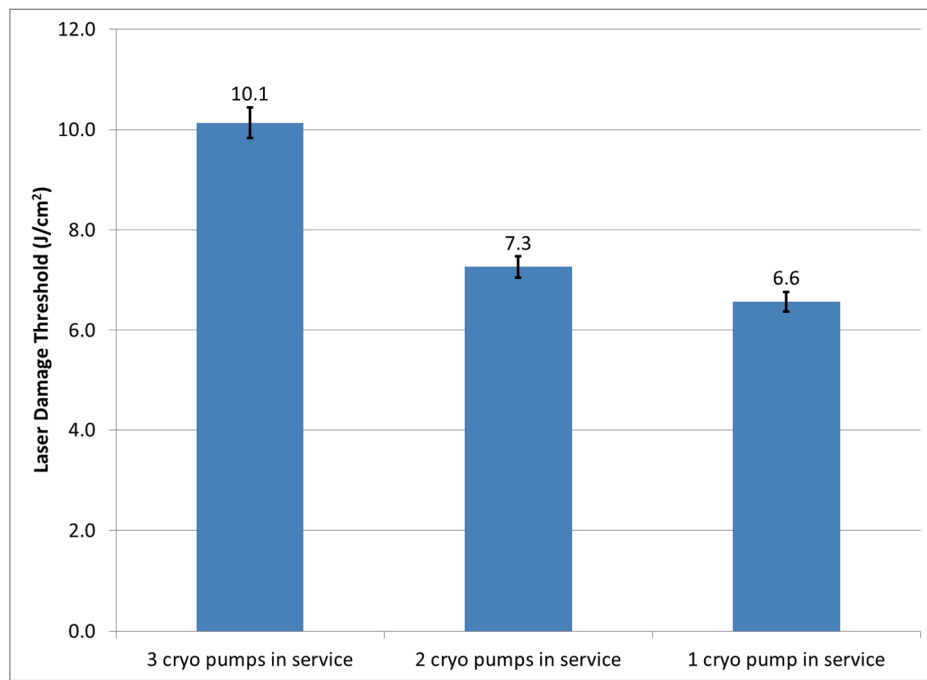


Figure 5: LIDT data of the AR coatings at 532 nm and normal incidence.

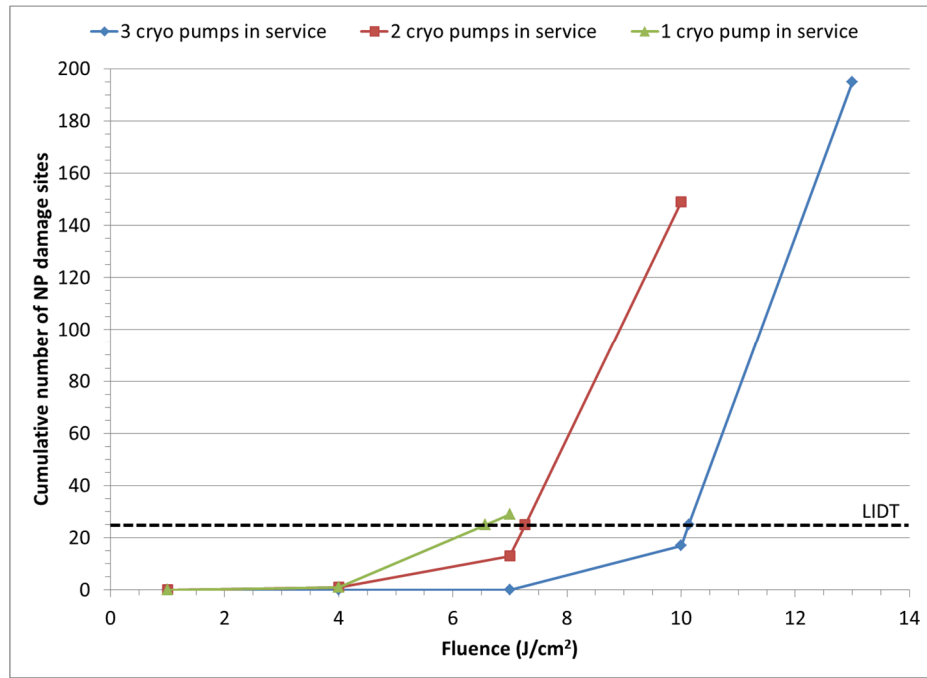


Figure 6: Cumulative number of non-propagating (NP) damage sites in the AR coatings for normal incidence at 532 nm.

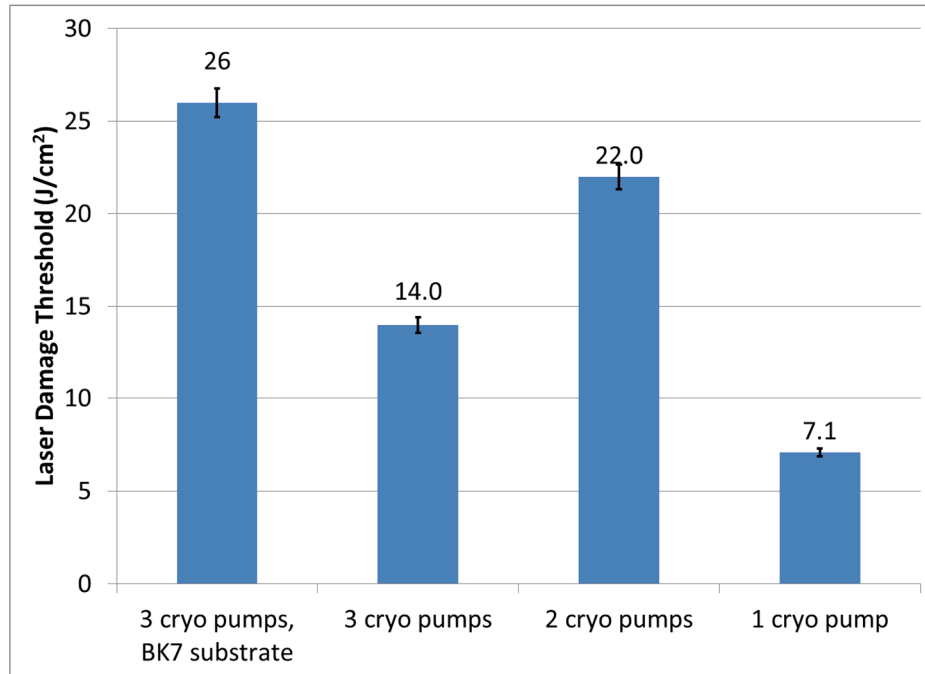


Figure 7: LIDT data of the HR coatings at 532 nm, 45° AOI, P-pol.

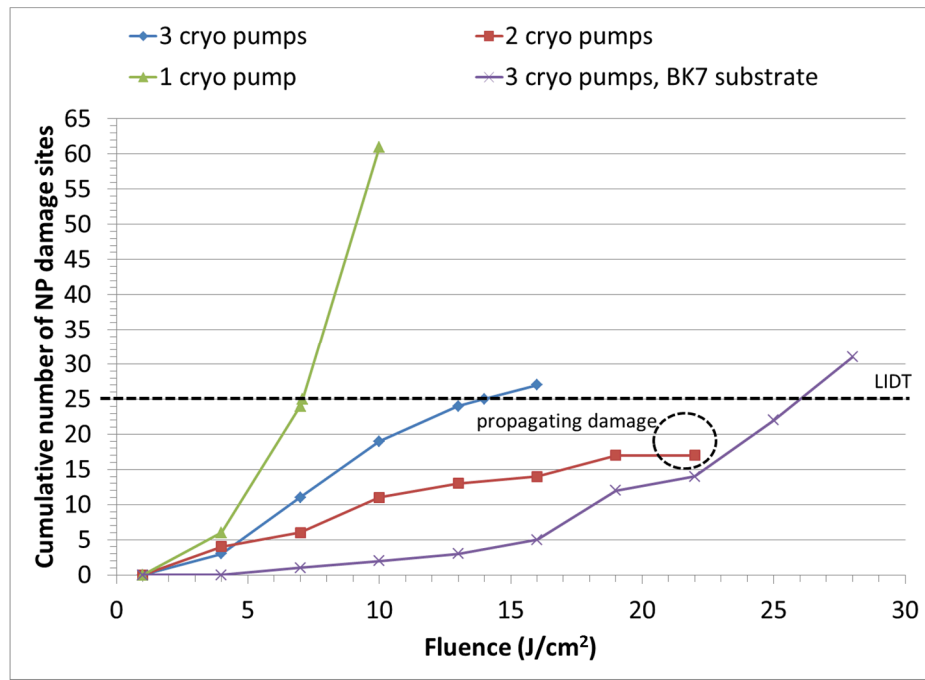


Figure 8: Cumulative number of non-propagating (NP) damage sites in the HR coatings at 532 nm, 45° AOI, P-pol.

5. CONCLUSION

This study addresses whether high LIDT coatings can be produced with reduced vacuum pumping capability in a coating chamber. In the case of both AR and HR coatings for 527 nm, reducing the number of cryo pumps in our coating chamber had a negative effect on the LIDT of the coatings, and

highlights the importance of adequate vacuum pumping speeds for achieving higher LIDTs. An increase in the number of non-propagating defects is responsible for reducing the LIDTs of coatings deposited with fewer cryo pumps, which is indicative of less effective oxidation of Hf, or the presence of excess particles in the chamber that act as contamination in the coatings. Whether or not the lower LIDTs caused by fewer vacuum pumps render an optic unusable depends on the particular application, and we found that the decline in LIDT due to fewer cryo pumps in operation is more drastic for HR coatings ($26 \text{ J/cm}^2 \rightarrow 7.1 \text{ J/cm}^2$) than AR coatings ($10.1 \text{ J/cm}^2 \rightarrow 6.6 \text{ J/cm}^2$).

The number of cryo pumps in operation affected the spectral characteristics of our HR coatings. We have evidence that the partial pressure of the O_2 backfill supplied during HfO_2 deposition was reduced due to the presence of excess particles in the chamber caused by lower vacuum pumping speeds. Lower O_2 partial pressure may be less effective at oxidizing Hf, which can increase the index of refraction of the HfO_2 layers and therefore affect the spectral characteristics of the coating. In addition, less effective oxidation of Hf can lead to lower LIDTs because Hf is highly absorbing. Fortunately, the spectral characteristics of the AR coatings were not affected by reducing cryo pumps, but this is likely because the AR coatings were too thin for slight index of refraction errors to amount to noticeable spectral problems.

This study has shown that increasing the vacuum pumping capability in a coating chamber can improve the LIDT of optical coatings. For us, this means depositing coatings with all 3 of our cryo pumps in operation. But even under these optimal conditions, the LIDTs were still dominated by NP defects. Therefore, further improvements to our LIDTs will become possible by determining the source of these defects and learning how to mitigate them.

ACKNOWLEDGEMENTS

Sandia National Laboratories is a multi-program laboratory managed and operated by Sandia Corporation, a wholly owned subsidiary of Lockheed Martin Corporation, for the U. S. Department of Energy's National Nuclear Security Administration under contract AC04-94AL85000.

REFERENCE

- [1] www.z-beamlet.sandia.gov
- [2] J. Bellum, et al, "Meeting thin film design and production challenges for laser damage resistant optical coatings at the Sandia Large Optics Coating Operation," in *Proc. SPIE Laser-Induced Damage in Optical Materials*, vol. 7504, pp. 75041C-1 – 75041C-13 (2009).
- [3] J. Bellum, et al, "Design and laser damage properties of a dichroic beam combiner coating for 22.5° incidence and S polarization with high transmission at 527 nm and high reflection at 1054 nm," submitted to *Proc. SPIE Laser-Induced Damage in Optical Materials* (2015).
- [4] J. Bellum, et al, "Comparisons between laser damage and optical electric field behaviors for hafnia/silica antireflection coatings," *Applied Optics*, vol. 50, no. 9, pp. C340-C348 (2011).
- [5] J. Bellum, "Reactive ion-assisted deposition of e-beam evaporated titanium for high refractive index TiO_2 layers and laser damage resistant, broad bandwidth, high reflection coatings" *Applied Optics*, vol. 53, no. 4, pp. A205-A211 (2014).

- [6] E. Field, et al, “Laser Damage Comparisons of Broad-Bandwidth, High-Reflection Optical Coatings Containing TiO_2 , Nb_2O_5 , or Ta_2O_5 High Index Layers,” in *Proc. SPIE Laser-Induced Damage in Optical Materials*, vol. 8885, pp. 88851X-1 – 88851X-8 (2013).
- [7] E. Field, et al, “Repair of a Mirror Coating on a Large Optic for High Laser Damage Applications using Ion Milling and Over-Coating Methods,” in *Proc. SPIE Laser-Induced Damage in Optical Materials*, vol. 9237, pp. 92371-1 – 92371-13 (2014).
- [8] E. Field, et al, “Impact of different cleaning processes on the laser damage threshold of antireflection coatings for Z-Backlighter optics at Sandia National Laboratories,” *Optical Engineering*, vol. 53, no. 12, pp. 122516-1 – 112516-8 (2014).
- [9] J. Bellum, et al, “Laser damage by ns and sub-ps pulses on hafnia/silica anti-reflection coatings on fused silica double-sided polished using zirconia or ceria and washed with or without an alumina wash step,” in *Proc. of SPIE Laser-Induced Damage in Optical Materials*, vol. 7842, pp. 784208-1 – 784208-10 (2010).
- [10] S. Liukaitytė, et al, “Effect of conventional fused silica preparation and deposition techniques on surface roughness, scattering and laser damage resistance,” in *Proc. of SPIE Laser-Induced Damage in Optical Materials*, vol. 8530, pp. 853027-1 – 853027-12 (2012).
- [11] B. Mangote, et al, “Femtosecond laser damage resistance of oxide and mixture oxide optical coatings,” *Optics Letters*, vol. 37, issue 9, pp. 1478-1480 (2012).
- [12] L. Gallais, et al, “Laser damage resistance of hafnia thin films deposited by electron beam deposition, reactive low voltage ion plating, and dual ion beam sputtering,” *Applied Optics*, vol. 47, no 13, pp. C107-C113 (2008).
- [13] L. Gallais, et al, “Laser-induced damage of hafnia coatings as a function of pulse duration in the femtosecond to nanosecond range,” *Applied Optics*, vol. 50, Issue 9, pp. C178-C187 (2011).
- [14] C. J. Stoltz and F. Y. Genin, “Laser Resistant Coatings,” in *Optical Interference Coatings*, N. B. Kaiser and H. K. Pulker, Eds. Berlin Heidelberg, Germany: Springer-Verlag, pp. 309-333 (2003).
- [15] www.spicatech.com
- [16] J. Wolfe, et al, “Small Optics Laser Damage Test Procedure”, Tech. Rep. MEL01-013-0D (Lawrence Livermore National Laboratory, Livermore, CA 2005).